Bartell, L. S., Roth, E. A., Hollowell, C. D., Kuchitsu, K. & Young, J. E. (1965). *J. Chem. Phys.* **42**, 2683–2686.

Durant, F., Bufkens, F., Lefevre, F., Evrard, G. & Michel, A. (1985). *Acta Cryst.* C**41**, 243–246.

Fallon, G. D., Fitzmaurice, N. J., Jackson, W. R. & Perlmutter, P. (1986). *Acta Cryst.* C**42**, 1654–1655.

Fonseca, I., Martínez-Carrera, S. & García-Blanco, S. (1986). *Acta Cryst.* C**42**, 1792–1794.

International Tables for X-ray Crystallography (1974). Vol. IV. Birmingham: Kynoch Press. (Present distributor Kluwer Academic Publishers, Dordrecht.)

Klokol, G. V., Sharanina, L. G., Nesterov, V. N., Shklover, V. E., Sharanin, Yu. A. & Struchkov, Yu. T. (1987). *Zh. Org. Khim.* **23**, 412–421.

Main, P., Hull, S. E., Lessinger, L., Germain, G., Declercq, J.-P. & Woolfson, M. M. (1978). *MULTAN78. A System of Computer Programs for the Automatic Solution of Crystal Structures from X-ray Diffraction Data.* Univs. of York, England, and Louvain, Belgium.

Marchalín, Š., Pavlíková, F. & Ilavský, D. (1989). *Collect. Czech. Chem. Commun.* **54**, 1336.

Sharanina, L. G., Nesterov, V. N., Klokol, G. V., Rodinovskaya, L. A., Shklover, V. E., Sharanin, Yu. A., Struchkov, Yu. T. & Promonenkov, V. K. (1986). *Zh. Org. Khim.* **22**, 1315–1322.

Ukhin, L. Yu., Bessonov, V. V., Yanovskii, A. I., Timofeeva, T. V., Furmanova, N. G. & Struchkov, Yu. T. (1980). *Khim. Geterotsikl. Soedin.* pp. 461–467.

Acta Cryst. (1990). C**46**, 791–797

Structures of Four Pyrazolo[3,4-*b*]pyridine Nucleosides

By Steven B. Larson,* Yogesh S. Sanghvi, Ganapathi R. Revankar and Roland K. Robins

ICN-Nucleic Acid Research Institute, 3300 *Hyland Avenue Costa Mesa, CA* 92626, *USA*

(*Received* 13 *March* 1989; *accepted* 13 *July* 1989)

Abstract. 4-Methoxy-1-(2-deoxy-β-D-*erythro*-pentofuranosyl)-1*H*-pyrazolo[3,4-*b*]pyridine (1), $C_{12}H_{15}N_3O_4$, M_r = 265·27, orthorhombic, $P2_12_12_1$, a = 6·9930 (10), b = 9·231 (2), c = 19·119 (4) Å, V = 1234·2 (4) Å^3, Z = 4, D_x = 1·428 g cm^{-3}, Cu $K\alpha$ (λ = 1·54178 Å), μ = 8·718 cm^{-1}, $F(000)$ = 560, T = 295 K, R = 0·0361 for 2330 reflections ($F \geq 4\sigma_F$); 1-(2-deoxy-β-D-*erythro*-pentofuranosyl)-1*H*-pyrazolo[3,4-*b*]pyridin-4(7*H*)-one (2), $C_{11}H_{13}N_3O_4$, M_r = 251·24, monoclinic, $C2$, a = 17·506 (3), b = 8·512 (2), c = 7·941 (3) Å, β = 110·59 (3)°, V = 1107·7 (6) Å^3, Z = 4, D_x = 1·506 g cm^{-3}, Cu $K\alpha$ (λ = 1·54178 Å), μ = 9·406 cm^{-1}, $F(000)$ = 528, T = 295 K, R = 0·0369 for 1874 reflections ($F \geq 4\sigma_F$); 1-β-D-arabinofuranosyl-1*H*-pyrazolo[3,4-*b*]pyridin-4(7*H*)-one (3) dihydrate, $C_{11}H_{13}N_3O_5.2H_2O$, M_r = 303·27, monoclinic, $P2_1$, a = 4·8604 (3), b = 12·6573 (15), c = 10·9802 (17) Å, β = 91·17 (6)°, V = 675·36 (13) Å^3, Z = 2, D_x = 1·491 g cm^{-3}, Cu $K\alpha$ (λ = 1·54178 Å), μ = 10·325 cm^{-1}, $F(000)$ = 320, T = 295 K, R = 0·0291 for 2692 reflections ($F \geq 4\sigma_F$); 1-β-D-ribofuranosyl-1*H*-pyrazolo[3,4-*b*]pyridine (4), $C_{11}H_{13}N_3O_4$, M_r = 251·24, orthorhombic, $P2_12_12_1$, a = 6·9252 (6), b = 8·288 (6), c = 19·431 (3) Å, V = 1115·2 (8) Å^3, Z = 4, D_x = 1·496 g cm^{-3}, Cu $K\alpha$ (λ = 1·54178 Å), μ = 9·342 cm^{-1}, $F(000)$ = 528, T = 295 K, R = 0·0298 for 2045 reflections ($F \geq 4\sigma_F$). The 4-hydroxy compounds (2) and (3) exist as the oxo tautomers with N7 protonated. The pyrazole–pyridine dihedral angles are 0·44 (7), 1·00 (13), 0·47 (7) and 0·95 (6)° for (1)–(4), respectively. Compounds (1) and (3) are in the *syn* conformation with stabilizing intramolecular O5′···N7 hydrogen bonds; (2) and (4) are in the *anti* conformation. The sugar moieties have conformations of ^2E (C2′-*endo*), $_4T^3$ (C4′-*exo*), $^3T_4$ (C3′-*endo*) and $_3T^2$ (C3′-*exo*) for (1)-(4), respectively. Compound (4) has nearly complete, antiparallel base stacking.

Introduction. For two decades the search for beneficial drugs has included the synthesis and biological evaluation of nucleosides containing modified purine rings (Revankar, Gupta, Adams, Dalley, McKernan, Cook, Canonico & Robins, 1984; Meyer, Revankar, Cook, Ehler, Schweizer & Robins, 1980; Cline, Panzica & Townsend, 1978). The pyrazolo[3,4-*b*]pyridine nucleosides presented in this study [(1)–(4)] were synthesized (Sanghvi, Larson, Willis, Robins & Revankar, 1989) as examples of nitrogen modification in the purine ring system. These compounds possess the 1-deaza feature of 1-deazaadenosine [(5)] and the pyrazole ring in place of the imidazole ring as found in 1-β-D-ribofuranosylpyrazolo[3,4-*d*]pyrimidin-4(5*H*)-one [(6), allopurinol ribonucleoside]. Allopurinol ribonucleoside (Lichtenthaler & Cuny, 1981; Cottam, Petrie, McKernan, Goebel, Dalley, Davidson, Robins & Revankar, 1984) and 1-deazaadenosine (Itoh, Kitano & Mizuno, 1972; Cristalli, Franchetti, Grifantini, Vittori, Bordoni & Geroni, 1987) possess significant chemotherapeutic proper-

---

* Author to whom correspondence should be addressed.

0108-2701/90/050791-07$03.00

ties; recently the latter has been shown to have a high affinity for adenosine receptors (Cristalli, Franchetti, Grifantini, Vittori, Klotz & Lohse, 1988). Little or no antiviral and antitumor activity results from combining these features in the heterocycle. The structural studies were initiated to verify the site of glycosylation, the anomeric configuration and the general conformational features of representatives of the 2′-deoxyribofuranosides [(1), (2)], the arabinofuranosides [(3)] and the ribofuranosides [(4)] of this class of purine analogs.

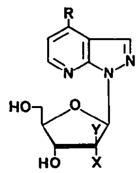

(1) $R = OCH_3$; $X = Y = H$
(2) $R = OH$;* $X = Y = H$
(3) $R = OH$;* $X = H$; $Y = OH$
(4) $R = H$; $X = OH$; $Y = H$
*As oxo tautomer

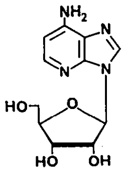

(5)
1-Deazaadenosine

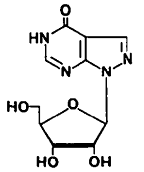

(6)
Allopurinol ribonucleoside

Experimental. Compounds (1)–(4) were synthesized by the sodium salt glycosylation procedure utilizing the appropriate heterocycle and halogenose followed by removal of the protecting groups as recently reported (Sanghvi *et al.*, 1989). Crystals of (1) grew from ethanol/ethyl acetate (9:1, *v*/*v*) as prisms. Crystals of (2) grew from ethanol/water (1:1, *v*/*v*) as long, thin plates. Crystals of (3) and (4) grew from ethanol, (3) as irregular needles and (4) as hexagonal needles. Table 1 summarizes data collection and refinement of all structures. Data for each compound were corrected for Lorentz, polarization, decay and absorption. The absorption corrections were based on measurements of crystal faces to define the shape and size of the crystals used for data collection.

Crystallographic coordinates of all non-H atoms of each compound [including the two water molecules in (3)] were determined with *SHELXS*86 (Sheldrick, 1986). H-atom positions for each compound were obtained from a difference map as peaks of density 0·36–0·77, 0·55–0·90, 0·28–0·87 and 0·50–1·05 e Å^{-3} and at *R* values of 0·066, 0·061, 0·053 and 0·059 for (1)–(4), respectively. All positional and thermal parameters were refined (only H atoms were treated isotropically) for each structure using the program *SHELX*76 (Sheldrick, 1976). Scattering factors and anomalous-dispersion corrections were taken from *International Tables for X-ray Crystallography* (1974) except those of H which were taken from Stewart, Davidson & Simpson (1965). Data were reduced with *SDP-Plus* (Frenz, 1985); least-squares-planes program from Cordes (1983). Figures were drawn with *ORTEP*II (Johnson, 1976); all thermal ellipsoids are drawn at the 50% probability level.*

Discussion. The atomic coordinates are listed in Tables 2–5; bond lengths and bond angles are listed in Table 6. The atom labeling is shown in Figs. 1–4 for compounds (1)–(4), respectively. The site of glycosylation at N1 of the pyrazolo[3,4-*b*]pyridine ring system and the anomeric configuration as β were confirmed for all nucleosides studied.

The aglycon moiety. The 4-hydroxy compounds [(2) and (3)] exist in the solid state as the oxo tautomer protonated at N7. In (3) this proton is donated to O5′ intramolecularly whereas in (2) it is donated to O5′ intermolecularly. In each structure, the pyrazolopyridine ring systems are essentially planar (r.m.s. deviations less than 0·012 Å for each structure); the dihedral angles between the planes of the fused pyrazole and pyridine rings are 0·44 (7)° for (1), 1·00 (13)° for (2), 0·47 (7)° for (3), and 0·95 (6)° for (4). The methoxy group in (1) is nearly coplanar [dihedral angle of 0·56 (9)°] with the pyrazolopyridine plane, such that the methyl group is *trans* to the pyrazole ring. The 4-oxopyrazolopyridine systems of (2) and (3) are essentially identical but significantly different from the pyrazolopyridine systems of (1) and (4), which, despite the lack of a 4-methoxy group in (4), are nearly identical. In comparison to (1) and (4), the conjugated group at C4 in (2) and (3) lengthens the C4—C9, C4—C5 and C6—N7 bonds and shortens the C5—C6 bond in agreement with the predominant canonical form of these molecules. The N2—C3 and N1—N2 bonds are slightly longer in the 4-oxo compounds (2) and (3).

The glycosyl linkage and overall conformation. The glycosyl bonds are 1·449 (2) and 1·452 (3) Å for the 2′-deoxy compounds [(1) and (2)], 1·462 (2) Å for the arabinose structure [(3)] and 1·441 (2) Å for the ribose compound [(4)]. Atom C1′ in (1) is nearly coplanar [deviation: −0·012 (2) Å] with the heterocycle whereas in (2), (3) and (4) the deviations are −0·188 (3), 0·2377 (15) and 0·163 (2) Å, respectively. Table 7 tabulates conformational properties. Structures (1) and (3) are in the *syn* conformation whereas the other two are in *anti* conformations. The two *syn* structures are stabilized by intramolecular hydrogen bonds (Table 8), but the bond in (1) is O5′—H···N7 whereas in (3) the bond is N7—H···O5′. There is no intramolecular hydrogen bonding in (2) or (4).

---

* Tables of anisotropic thermal parameters, bond lengths and angles involving H atoms, torsion angles, least-squares planes and structure factor amplitudes have been deposited with the British Library Document Supply Centre as Supplementary Publication No. SUP 52449 (46 pp.). Copies may be obtained through The Technical Editor, International Union of Crystallography, 5 Abbey Square, Chester CH1 2HU, England.

Table 1. *Crystallographic summary for* (1), (2), (3) *and* (4)

	(1)	(2)	(3)	(4)
Data collection[a,b]				
Mode	ω–2θ scan			
Background	Scan 0·25 times scan range before and after scan			
Scan range (°)	1·0 + 0·15tanθ	1·0 + 0·15tanθ	0·80 + 0·15tanθ	0·80 + 0·15tanθ
Scan rate (° min^{-1})	1·3–8·2	1·3–16·5	1·3–16·5	1·3–16·5
2θ range (°)	3–152	3–152	3–152	3–152
Exposure time (h)	38·4	29·6	22·2	55·1
Stability correction range on I	1·000–1·041	1·000–1·005	1·000–1·002	1·000–1·000
Range in *hkl*, min.	0,0,−24	0,−10,−9	0,−15,−13	0,−10,−24
max.	8,11,24	22,10,9	6,15,13	8,10,24
Total reflections measured, unique	2927, 2565	2377, 2250	3112, 2784	5025, 2332
R_{int}	0·026	0·019	0·013	0·028
Crystal dimensions (mm)	0·35 × 0·30 × 0·165	0·425 × 0·22 × 0·035	0·42 × 0·175 × 0·15	0·30 × 0·14 × 0·095
Crystal volume (mm^3)	0·0116	0·00350	0·00820	0·00292
Crystal faces	{001},{011},{102} 111,210,1$\bar{1}$0	{100},{010},{001}	{011},100,$\bar{1}$01 $\bar{1}$0$\bar{1}$,010	{011},{001} 100,$\bar{1}$02
Transmission factor range	0·745–0·881	0·774–0·967	0·580–0·887	0·818–0·934
Structure refinement[c]				
Reflections used, m ($F \geq 4\sigma_F$)	2330	1874	2692	2045
No. of variables, n	233	215	258	216
Extinction parameter	1·3 (2) × 10^{-6}	3·8 (10) × 10^{-7}	3·6 (4) × 10^{-6}	1·8 (2) × 10^{-6}
Goodness of fit, S	1·576	1·391	1·567	1·333
R, wR	0·0361, 0·0476	0·0369, 0·0466	0·0291, 0·0425	0·0298, 0·0381
R for all data	0·0423	0·0556	0·0312	0·0401
Max. Δ/σ	0·002	0·007	0·001	0·003
Max., min. ρ in ΔF map (e Å^{-3})	0·25, −0·26	0·30, −0·31	0·34, −0·28	0·36, −0·23

Notes: (*a*) Unit-cell parameters were obtained by least-squares refinement of the setting angles of 25 reflections with $55·3 < 2\theta < 59·1°$ for (1), $46·6 < 2\theta < 57·2°$ for (2), $52·9 < 2\theta < 59·7°$ for (3), and $39·6 < 2\theta < 58·4°$ for (4). (*b*) Enraf–Nonius CAD-4 diffractometer with a graphite monochromator was used. Data reduction was accomplished with the *SDP-Plus* software (Frenz, 1985). Crystal and instrument stabilities were monitored by remeasurement of three check reflections every hour [(1) 2,2,10, 25$\bar{2}$ and 4$\bar{2}$2; (2) 62$\bar{4}$, $\overline{24}$2 and 531; (3) 14$\bar{5}$, 253 and 1$\bar{5}$4; (4)119, 12$\bar{8}$ and 4$\bar{1}$2]. A linear fit of the intensities of these reflections was used to correct the data . (*c*) Function minimized was $\sum w(|F_o| - |F_c|)^2$, where $w^{-1} = (\sigma_F^2 + 0·0004F^2)$ was used for all structures. $R = \sum||F_o| - |F_c||/\sum|F_o|$; $wR = [\sum w(|F_o| - |F_c|)^2/\sum w|F_o|^2]^{1/2}$. $S = [\sum w(|F_o| - |F_c|)^2/(m - n)]^{1/2}$. $\sigma_F = F\sigma_I/2I$; $\sigma_I = [N_{pk} + N_{bg1} + N_{bg2}]^{1/2}$.

The sugar moiety. The conformational parameters (according to Altona & Sundaralingam, 1972) of the furanose moieties are given in Table 7. Each compound possesses a distinct sugar conformation. The C5′—O5′ side chains assume the *gauche*$^-$–*gauche* orientation only for the *syn* conformations; the others have the *gauche*$^+$–*trans* orientation. Although there are several significant differences in bond lengths of corresponding bonds in the four structures, bond lengths are generally consistent among them and all fall into normal ranges.

Packing. The hydrogen bonding in the four structures is detailed in Table 8 and illustrated in the packing diagrams of Figs. 5–8. The nucleoside base rings in the methoxy compound (1) are layered parallel to the *bc* plane with a separation of approximately 3·5 Å; however, the stacking is limited to sandwiching of the methoxy groups between pyridine rings of the two adjacent layers as suggested in Fig. 5. Thus, C11 is 3·554 (3) and 3·448 (3) Å from C8 atoms of adjacent molecules; C4, which is approximately on a 2_1 axis, is 3·503 (2) Å from both C4 atoms of adjacent pyridine rings. Both hydroxyl group hydrogens are involved in moderately strong hydrogen bonding as detailed in Table 8; O5′—H···N7 is an intramolecular hydrogen bond and O3′—H···O5′ is an intermolecular bond linking molecules along the *b* axis. A weak C6—H6···O3′ interaction appears likely.

The base rings in compound (2) are parallel to the (10$\bar{2}$) plane although the layering is staggered. The dimeric molecules about the twofold axis, which are reciprocally hydrogen bonded through N7—H···O5′ bonds, have base separation of approximately 4 Å, a distance dictated by the positioning of the sugar C5′—O5′ side chains which are involved in the hydrogen bonds. The base separation between adjacent dimeric units is less than 4 Å [closest interatomic distance is C9···C9 at 3·723 (4) Å] which suggests that there are no appreciable base stacking interactions in this structure. The dimers are linked along the *b* axis through pairs of strong O5′—H···O10 hydrogen bonds. Along the *a* axis the dimers are linked by a single O3′—H···N2 hydrogen bond of moderate strength.

Planes of the base rings related by unit translations along the *a* axis in the arabinoside (3) are separated by ~3·4 Å. There is no base stacking, although the base rings have close contacts with the C4—O10 bond (within 3·35 Å of C8) on one side of the base ring and O4′ (within 3·14 Å of C8) on the other side (Fig. 7*a*). Unlike the packing in nucleosides (1), (2) and (4), all bases do not lie in nearly parallel planes. This may result from the presence of the water of solvation in the lattice which forms a hydrogen-bonded chain parallel to the *a* axis. There are eight fairly strong [maximum H···*A* distance is 2·01 (4) Å] hydrogen bonds (including the intramolecular bond N7—H···O5′) which involve all of the amino and hydroxyl protons. Only the 4-oxo compounds (2) and (3) exhibit hydrogen bonding interactions involving N2 which, in conjunction with the longer

Table 2. *Positional and isotropic thermal parameters* (Å^2) *for atoms in* (1)

	x	*y*	*z*	U/U_{eq}*
N1	0·8045 (3)	0·61109 (14)	0·44745 (7)	0·0478 (5)
N2	0·8123 (3)	0·6425 (2)	0·51711 (8)	0·0611 (6)
C3	0·8148 (4)	0·5171 (2)	0·54973 (10)	0·0591 (6)
C4	0·8072 (2)	0·2473 (2)	0·50511 (9)	0·0453 (5)
C5	0·8000 (3)	0·1760 (2)	0·44202 (10)	0·0496 (5)
C6	0·7925 (3)	0·2548 (2)	0·37924 (10)	0·0465 (5)
N7	0·7916 (2)	0·39863 (14)	0·37359 (7)	0·0419 (4)
C8	0·8025 (3)	0·4649 (2)	0·43639 (8)	0·0403 (4)
C9	0·8090 (3)	0·3997 (2)	0·50242 (9)	0·0446 (5)
O10	0·8128 (2)	0·1861 (2)	0·56878 (7)	0·0617 (5)
C11	0·8101 (4)	0·0297 (3)	0·5721 (2)	0·0686 (8)
C1′	0·8005 (3)	0·7280 (2)	0·39691 (9)	0·0466 (5)
C2′	0·9639 (3)	0·7293 (2)	0·34456 (10)	0·0474 (5)
C3′	0·8732 (3)	0·8089 (2)	0·28298 (9)	0·0435 (5)
C4′	0·6644 (3)	0·7632 (2)	0·28606 (9)	0·0428 (5)
C5′	0·6092 (3)	0·6424 (2)	0·23677 (11)	0·0515 (6)
O3′	0·8805 (3)	0·96236 (13)	0·29196 (8)	0·0586 (5)
O4′	0·6302 (2)	0·71467 (14)	0·35678 (6)	0·0474 (4)
O5′	0·7331 (2)	0·51995 (13)	0·24063 (7)	0·0517 (4)
H3	0·827 (4)	0·516 (3)	0·6029 (14)	0·076 (7)
H5	0·794 (4)	0·073 (2)	0·4399 (11)	0·058 (6)
H6	0·790 (3)	0·202 (2)	0·3349 (11)	0·055 (5)
H11*A*	0·689 (5)	−0·009 (3)	0·550 (2)	0·091 (9)
H11*B*	0·810 (5)	0·012 (3)	0·619 (2)	0·115 (12)
H11*C*	0·925 (4)	−0·006 (3)	0·5499 (15)	0·081 (8)
H1′	0·806 (3)	0·819 (2)	0·4200 (11)	0·055 (6)
H2′*A*	0·996 (3)	0·631 (2)	0·3285 (10)	0·046 (5)
H2′*B*	1·077 (4)	0·782 (3)	0·3618 (12)	0·068 (7)
H3′	0·933 (3)	0·781 (2)	0·2392 (11)	0·049 (6)
H4′	0·579 (3)	0·850 (2)	0·2767 (9)	0·039 (5)
H5′*A*	0·475 (4)	0·610 (3)	0·2459 (13)	0·064 (6)
H5′*B*	0·610 (4)	0·677 (3)	0·1888 (12)	0·067 (7)
H*O*3′	0·996 (5)	0·985 (3)	0·2898 (13)	0·068 (7)
H*O*5′	0·732 (4)	0·489 (3)	0·284 (2)	0·077 (8)

* For non-H atoms, U is $U_{eq} = \frac{1}{3}\sum_i\sum_j U_{ij}a_i^*a_j^*A_{ij}$, where A_{ij} is the dot product of the *i*th and *j*th direct-space unit-cell vectors.

Table 3. *Positional and isotropic thermal parameters* (Å^2) *for atoms in* (2)

	x	*y*	*z*	U/U_{eq}*
N1	0·54905 (11)	0·478741	0·2736 (3)	0·0382 (7)
N2	0·61603 (12)	0·5757 (4)	0·3133 (4)	0·0482 (9)
C3	0·58691 (15)	0·7209 (4)	0·2879 (4)	0·0477 (10)
C4	0·4395 (2)	0·8435 (4)	0·1929 (4)	0·0383 (8)
C5	0·3582 (2)	0·7808 (4)	0·1496 (4)	0·0422 (9)
C6	0·3429 (2)	0·6240 (4)	0·1479 (4)	0·0393 (9)
N7	0·40250 (11)	0·5128 (3)	0·1846 (3)	0·0345 (7)
C8	0·47999 (13)	0·5651 (4)	0·2296 (3)	0·0317 (7)
C9	0·50105 (14)	0·7231 (4)	0·2352 (3)	0·0356 (8)
O10	0·45478 (12)	0·9870 (3)	0·1950 (3)	0·0537 (9)
C1′	0·55913 (13)	0·3117 (3)	0·3115 (3)	0·0340 (8)
C2′	0·6187 (2)	0·2283 (4)	0·2388 (4)	0·0395 (9)
C3′	0·68842 (14)	0·1786 (4)	0·4078 (3)	0·0332 (8)
C4′	0·64683 (13)	0·1671 (3)	0·5461 (3)	0·0332 (8)
C5′	0·70264 (14)	0·1872 (4)	0·7372 (3)	0·0364 (8)
O3′	0·72442 (11)	0·0353 (3)	0·3817 (3)	0·0411 (6)
O4′	0·59058 (11)	0·2960 (3)	0·5016 (2)	0·0424 (6)
O5′	0·66029 (10)	0·2038 (3)	0·8605 (2)	0·0357 (6)
H3	0·624 (2)	0·802 (4)	0·306 (4)	0·049 (8)
H5	0·315 (2)	0·854 (4)	0·115 (4)	0·047 (9)
H6	0·291 (2)	0·572 (4)	0·120 (5)	0·059 (10)
H7	0·386 (2)	0·402 (4)	0·188 (4)	0·044 (8)
H1′	0·501 (2)	0·266 (3)	0·255 (3)	0·025 (6)
H2′*A*	0·592 (2)	0·136 (4)	0·160 (4)	0·046 (8)
H2′*B*	0·639 (2)	0·293 (4)	0·165 (4)	0·051 (8)
H3′	0·730 (2)	0·263 (4)	0·447 (5)	0·066 (11)
H4′	0·616 (2)	0·062 (4)	0·525 (4)	0·039 (7)
H5′*A*	0·738 (2)	0·277 (4)	0·748 (4)	0·043 (8)
H5′*B*	0·741 (2)	0·099 (4)	0·773 (4)	0·048 (8)
H*O*3′	0·770 (3)	0·032 (7)	0·480 (7)	0·11 (2)
H*O*5′	0·621 (2)	0·123 (5)	0·843 (5)	0·066 (11)

* For non-H atoms, U is $U_{eq} = \frac{1}{3}\sum_i\sum_j U_{ij}a_i^*a_j^*A_{ij}$, where A_{ij} is the dot product of the *i*th and *j*th direct-space unit-cell vectors.

Table 4. *Positional and isotropic thermal parameters* (Å^2) *for atoms in* (3)

	x	*y*	*z*	U/U_{eq}*
N1	0·9005 (2)	0·75	0·32251 (11)	0·0302 (3)
N2	0·8373 (3)	0·83482 (14)	0·39533 (12)	0·0379 (4)
C3	0·6361 (4)	0·8870 (2)	0·33935 (14)	0·0379 (4)
C4	0·3665 (3)	0·85951 (15)	0·13059 (13)	0·0328 (4)
C5	0·3717 (4)	0·7839 (2)	0·03314 (14)	0·0383 (4)
C6	0·5505 (3)	0·7014 (2)	0·03431 (13)	0·0362 (4)
N7	0·7352 (3)	0·68307 (14)	0·12624 (10)	0·0319 (3)
C8	0·7359 (3)	0·75107 (15)	0·22146 (12)	0·0273 (3)
C9	0·5620 (3)	0·83844 (15)	0·22698 (13)	0·0306 (4)
O10	0·2004 (3)	0·93674 (14)	0·13052 (11)	0·0430 (4)
C1′	1·0825 (3)	0·66840 (14)	0·37302 (12)	0·0282 (4)
C2′	0·9267 (3)	0·58207 (15)	0·44486 (12)	0·0293 (3)
C3′	0·8990 (3)	0·49391 (14)	0·35119 (13)	0·0284 (4)
C4′	1·1729 (3)	0·50285 (15)	0·28778 (13)	0·0293 (4)
C5′	1·1914 (3)	0·4529 (2)	0·16277 (15)	0·0374 (4)
O2′	0·6731 (2)	0·6146 (2)	0·49079 (10)	0·0407 (3)
O3′	0·8402 (3)	0·39340 (13)	0·39936 (11)	0·0403 (3)
O4′	1·2120 (2)	0·61591 (13)	0·27589 (8)	0·0304 (3)
O5′	0·9879 (3)	0·4988 (2)	0·08607 (12)	0·0545 (4)
O*W*1	0·2255 (3)	1·1154 (2)	0·26350 (12)	0·0492 (4)
O*W*2	0·7369 (4)	0·2175 (2)	0·2567 (2)	0·0628 (5)
H3	0·572 (5)	0·948 (2)	0·380 (2)	0·048 (6)
H5	0·252 (5)	0·788 (2)	−0·035 (2)	0·043 (5)
H6	0·565 (5)	0·653 (2)	−0·034 (2)	0·045 (6)
H7	0·838 (5)	0·623 (2)	0·122 (2)	0·056 (6)
H1′	1·214 (4)	0·706 (2)	0·426 (2)	0·035 (5)
H2′	1·055 (4)	0·5561 (14)	0·511 (2)	0·021 (4)
H3′	0·759 (4)	0·5073 (15)	0·295 (2)	0·023 (4)
H4′	1·322 (5)	0·474 (2)	0·340 (2)	0·041 (5)
H5′*A*	1·170 (4)	0·373 (2)	0·171 (2)	0·030 (4)
H5′*B*	1·385 (5)	0·466 (2)	0·130 (2)	0·050 (6)
H*O*2′	0·699 (5)	0·618 (2)	0·569 (3)	0·058 (7)
H*O*3′	0·958 (6)	0·382 (2)	0·459 (2)	0·059 (7)
H*O*5′	0·975 (6)	0·470 (2)	0·010 (3)	0·061 (8)
H*W*1*A*	0·205 (6)	1·048 (2)	0·231 (3)	0·062 (7)
H*W*1*B*	0·038 (10)	1·147 (3)	0·251 (4)	0·119 (13)
H*W*2*A*	0·725 (6)	0·266 (2)	0·312 (3)	0·060 (7)
H*W*2*B*	0·596 (9)	0·186 (4)	0·269 (3)	0·091 (12)

* For non-H atoms, U is $U_{eq} = \frac{1}{3}\sum_i\sum_j U_{ij}a_i^*a_j^*A_{ij}$, where A_{ij} is the dot product of the *i*th and *j*th direct-space unit-cell vectors.

Table 5. *Positional and isotropic thermal parameters* (Å^2) *for atoms in* (4)

	x	*y*	*z*	U/U_{eq}*
N1	0·8383 (2)	0·42225 (14)	0·59485 (6)	0·0314 (4)
N2	0·8336 (2)	0·5500 (2)	0·55004 (7)	0·0387 (4)
C3	0·8381 (3)	0·4880 (2)	0·48790 (8)	0·0414 (5)
C4	0·8471 (3)	0·1886 (2)	0·44287 (9)	0·0427 (5)
C5	0·8511 (3)	0·0356 (2)	0·46988 (9)	0·0441 (5)
C6	0·8561 (3)	0·0132 (2)	0·54141 (9)	0·0410 (5)
N7	0·8538 (2)	0·1314 (2)	0·58815 (6)	0·0343 (4)
C8	0·8438 (2)	0·2790 (2)	0·56011 (7)	0·0292 (4)
C9	0·8434 (3)	0·3166 (2)	0·48951 (8)	0·0356 (5)
C1′	0·8165 (2)	0·4479 (2)	0·66777 (7)	0·0265 (4)
C2′	0·9426 (2)	0·5868 (2)	0·69437 (8)	0·0283 (4)
C3′	0·8222 (2)	0·6512 (2)	0·75359 (8)	0·0308 (4)
C4′	0·6190 (2)	0·6356 (2)	0·72483 (8)	0·0280 (4)
C5′	0·5610 (2)	0·7780 (2)	0·68034 (10)	0·0370 (5)
O2′	1·1269 (2)	0·5319 (2)	0·71342 (7)	0·0410 (4)
O3′	0·8368 (2)	0·54893 (15)	0·81277 (6)	0·0379 (3)
O4′	0·6217 (2)	0·48807 (12)	0·68490 (6)	0·0300 (3)
O5′	0·3600 (2)	0·76720 (15)	0·66306 (7)	0·0388 (4)
H3	0·836 (3)	0·561 (2)	0·4474 (11)	0·045 (6)
H4	0·851 (3)	0·203 (3)	0·3937 (12)	0·054 (6)
H5	0·850 (4)	−0·060 (3)	0·4407 (12)	0·048 (6)
H6	0·860 (3)	−0·096 (2)	0·5582 (10)	0·037 (5)
H1′	0·846 (3)	0·346 (2)	0·6897 (8)	0·024 (4)
H2′	0·946 (3)	0·664 (2)	0·6579 (9)	0·025 (4)
H3′	0·860 (3)	0·762 (2)	0·7676 (11)	0·045 (5)
H4′	0·524 (3)	0·621 (2)	0·7613 (10)	0·030 (4)
H5′*A*	0·630 (4)	0·780 (3)	0·6346 (13)	0·065 (7)
H5′*B*	0·584 (3)	0·879 (3)	0·7046 (12)	0·050 (6)
H*O*2′	1·209 (4)	0·600 (3)	0·6983 (13)	0·055 (7)
H*O*3′	0·937 (4)	0·563 (3)	0·8348 (13)	0·056 (7)
H*O*5′	0·309 (4)	0·849 (3)	0·6744 (13)	0·058 (7)

* For non-H atoms, U is $U_{eq} = \frac{1}{3}\sum_i\sum_j U_{ij}a_i^*a_j^*A_{ij}$, where A_{ij} is the dot product of the *i*th and *j*th direct-space unit-cell vectors.

Table 6. *Bond lengths* (Å) *and angles* (°) *in* (1), (2), (3) *and* (4)

	(1)	(2)	(3)	(4)
N2—N1	1·364 (2)	1·377 (3)	1·377 (2)	1·371 (2)
C8—N1	1·366 (2)	1·352 (3)	1·355 (2)	1·366 (2)
C1′—N1	1·449 (2)	1·452 (3)	1·462 (2)	1·441 (2)
C3—N2	1·315 (2)	1·325 (5)	1·321 (2)	1·312 (2)
C9—C3	1·412 (2)	1·411 (3)	1·418 (2)	1·421 (3)
C5—C4	1·375 (3)	1·444 (4)	1·436 (2)	1·373 (3)
C9—C4	1·408 (2)	1·438 (4)	1·433 (2)	1·395 (3)
C6—C5	1·404 (3)	1·360 (5)	1·358 (3)	1·403 (2)
N7—C6	1·332 (2)	1·362 (4)	1·357 (2)	1·336 (2)
C8—N7	1·350 (2)	1·351 (3)	1·354 (2)	1·341 (2)
C9—C8	1·399 (2)	1·391 (4)	1·394 (2)	1·407 (2)
C2′—C1′	1·519 (3)	1·533 (4)	1·554 (2)	1·534 (2)
O4′—C1′	1·422 (2)	1·420 (3)	1·415 (2)	1·429 (2)
C3′—C2′	1·526 (3)	1·522 (3)	1·522 (2)	1·518 (2)
C4′—C3′	1·521 (3)	1·519 (4)	1·519 (2)	1·519 (2)
O3′—C3′	1·428 (2)	1·421 (4)	1·409 (2)	1·432 (2)
C5′—C4′	1·511 (3)	1·498 (3)	1·515 (2)	1·517 (2)
O4′—C4′	1·444 (2)	1·433 (4)	1·450 (2)	1·448 (2)
O5′—C5′	1·426 (2)	1·428 (4)	1·411 (2)	1·434 (2)
O10—C4	1·343 (2)	1·250 (4)	1·268 (2)	—
C11—O10	1·445 (3)	—	—	—
O2′—C2′	—	—	1·403 (2)	1·405 (2)
N2—N1—C8	111·20 (13)	110·2 (2)	109·43 (11)	110·96 (13)
C8—N1—C1′	129·24 (14)	128·2 (2)	131·34 (11)	128·11 (12)
C1′—N1—N2	119·56 (13)	120·6 (2)	118·10 (12)	120·53 (12)
C3—N2—N1	106·03 (14)	105·9 (2)	106·95 (13)	106·34 (14)
C9—C3—N2	111·8 (2)	111·7 (3)	111·1 (2)	111·82 (14)
C5—C4—C9	116·5 (2)	112·7 (3)	113·9 (2)	117·0 (2)
C6—C5—C4	120·2 (2)	122·7 (3)	121·74 (14)	120·1 (2)
N7—C6—C5	125·9 (2)	123·1 (2)	123·5 (2)	125·2 (2)
C8—N7—C6	112·27 (14)	116·7 (3)	117·2 (2)	113·17 (14)
C9—C8—N1	106·55 (14)	108·3 (2)	108·71 (13)	106·83 (13)
C9—C8—N7	127·58 (14)	123·9 (2)	123·09 (13)	126·75 (14)
N1—C8—N7	125·85 (14)	127·8 (3)	128·18 (14)	126·39 (13)
C3—C9—C4	138·1 (2)	135·3 (3)	135·6 (2)	138·2 (2)
C3—C9—C8	104·41 (14)	103·9 (2)	103·80 (13)	104·04 (13)
C4—C9—C8	117·53 (15)	120·9 (2)	120·60 (14)	117·7 (2)
C2′—C1′—O4′	105·97 (14)	107·2 (2)	106·34 (14)	106·51 (11)
C2′—C1′—N1	115·5 (2)	115·1 (2)	113·07 (11)	112·48 (12)
O4′—C1′—N1	108·17 (15)	106·6 (2)	108·71 (11)	111·26 (12)
C3′—C2′—C1′	101·5 (2)	103·7 (2)	102·12 (11)	101·93 (12)
C4′—C3′—O3′	107·74 (15)	113·6 (2)	115·19 (14)	108·08 (13)
C4′—C3′—C2′	103·63 (14)	102·5 (2)	100·88 (12)	101·53 (12)
O3′—C3′—C2′	111·71 (15)	111·7 (2)	115·09 (12)	111·18 (13)
C5′—C4′—O4′	108·22 (14)	108·0 (2)	108·65 (13)	110·78 (13)
C5′—C4′—C3′	115·20 (15)	114·7 (2)	116·91 (13)	112·88 (13)
O4′—C4′—C3′	106·32 (14)	103·6 (2)	103·43 (13)	104·91 (12)
O5′—C5′—C4′	113·4 (2)	113·3 (2)	108·40 (15)	110·00 (13)
C1′—O4′—C4′	109·87 (13)	108·0 (2)	109·55 (11)	109·47 (11)
C9—C4—O10	116·9 (2)	123·7 (2)	123·8 (2)	—
O10—C4—C5	126·6 (2)	123·5 (3)	122·29 (14)	—
C11—O10—C4	117·4 (2)	—	—	—
C3′—C2′—O2′	—	—	113·06 (12)	114·41 (13)
O2′—C2′—C1′	—	—	114·7 (2)	111·29 (13)

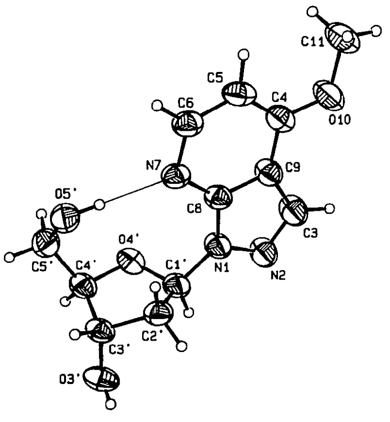

Fig. 1. Perspective drawing of (1) illustrating atom labeling and the O5′—H···N7 intramolecular hydrogen bond (thin line).

N2—C3 and N1—N2 bond lengths in these two structures compared to (1) and (4), suggests greater electron density at N2 in the former two nucleosides.

The riboside (4) has the most complete base stacking of the four compounds studied (Fig. 8*a*). The base rings are parallel to the *bc* plane as in (1), stacked in antiparallel fashion along the 2_1 axes perpendicular to this plane, which axes coincide with the long axis of the crystalline needle; thus, the stacks form rows parallel to the *ab* plane between

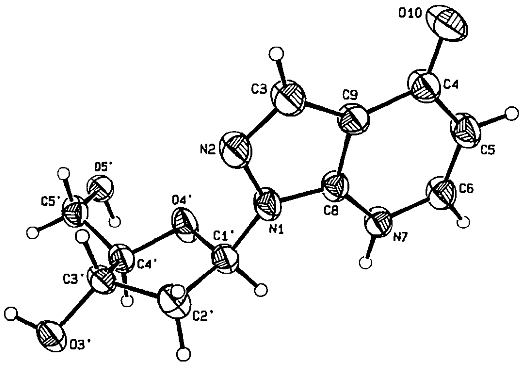

Fig. 2. Perspective drawing of (2) showing atom labeling.

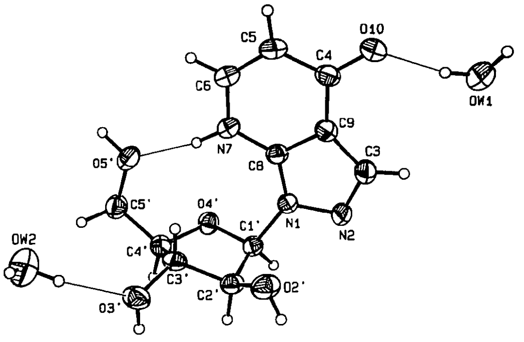

Fig. 3. Perspective drawing of (3) illustrating atom labeling and the N7—H···O5′ intramolecular hydrogen bond (thin line). Also included are the two hydrogen-bonded waters of solvation.

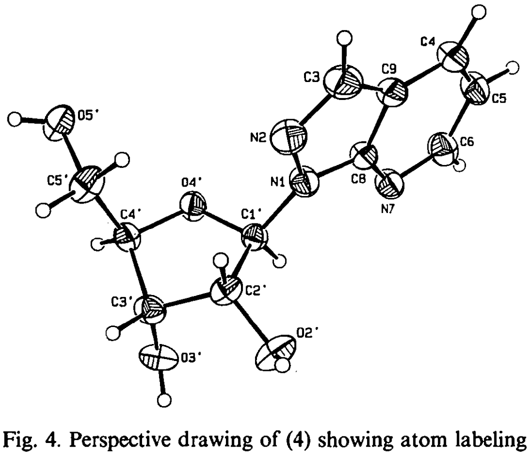

Fig. 4. Perspective drawing of (4) showing atom labeling.

Table 7. *Selected torsion angles* (°) *and conformational parameters in* (1), (2), (3) *and* (4)

		(1)	(2)	(3)	(4)
θ_0	C1′—C2′—C3′—C4′	−33·2 (2)	25·4 (3)	37·13 (14)	−37·93 (14)
θ_1	C2′—C3′—C4′—O4′	21·2 (2)	−37·8 (3)	−41·38 (13)	36·46 (14)
θ_2	C3′—C4′—O4′—C1′	·4 (2)	36·5 (3)	29·79 (13)	−20·28 (14)
θ_3	C4′—O4′—C1′—C2′	−22·2 (2)	−20·0 (3)	−5·59 (13)	−4·4 (2)
θ_4	O4′—C1′—C2′—C3′	34·4 (2)	−4·6 (3)	−20·60 (13)	26·99 (14)
χ	O4′—C1′—N1—N2	−120·9 (2)	67·7 (3)	−155·55 (12)	72·7 (2)
χ'	O4′—C1′—N1—C8	59·4 (3)	−99·6 (3)	38·0 (2)	−99·4 (2)
φ_{OO}	O4′—C4′—C5′—O5′	−68·6 (2)	54·6 (3)	−58·6 (2)	70·9 (2)
φ_{CO}	C3′—C4′—C5′—O5′	50·2 (2)	169·5 (3)	57·9 (2)	−171·78 (13)
Glysosidic conformation		*syn*	*anti*	*syn*	*anti*
P (°) pseudorotation angle*		160·7	48·9	26·2	192·3
τ_m (°) amplitude of pucker*		35·2	38·7	41·4	38·8
Sugar conformation*		C_2-*endo*	C_4-*exo*	C_3-*endo*	C_3-*exo*
		^2E	$_4T^3$	$^3T_4$	$_3T^2$
C5′—O5′ orientation		*gg*	*gt*	*gg*	*gt*

* See Altona & Sundaralingam (1972).

Table 8. *Hydrogen bonding in* (1), (2), (3) *and* (4)

D	—H	··· A	Symmetry of A relative to D	d(D···A) (Å)	d(H···A) (Å)	∠(D—H···A) (°)
(1)						
C6	H6	O3′	$x, y-1, z$	3·234 (2)	2·45 (2)	137· (2)
O3′	HO3′	O5′	$2-x, 0·5+y, 0·5-z$	2·824 (2)	2·01 (3)	165· (2)
O5′	HO5′	N7	x, y, z	2·808 (2)	1·94 (3)	165· (3)
(2)						
N7	H7	O5′	$1-x, y, 1-z$	2·825 (4)	1·85 (4)	166· (3)
O3′	HO3′	N2	$1·5-x, y-0·5, 1-z$	3·005 (3)	2·12 (6)	167· (5)
O5′	HO5′	O10	$1-x, y-1, 1-z$	2·652 (3)	1·71 (4)	176· (4)
(3)						
N7	H7	O5′	x, y, z	2·678 (2)	1·78 (3)	167· (2)
O2′	HO2′	OW1	$1-x, y-0·5, 1-z$	2·733 (2)	1·87 (3)	175· (3)
O3′	HO3′	N2	$2-x, y-0·5, 1-z$	2·819 (2)	1·96 (3)	167· (3)
O5′	HO5′	O10	$1-x, y-0·5, -z$	2·650 (2)	1·80 (3)	154· (3)
OW1	HW1A	O10	x, y, z	2·693 (2)	1·79 (3)	163· (3)
OW1	HW1B	OW2	$x-1, y+1, z$	2·704 (2)	1·72 (5)	168· (4)
OW2	HW2A	O3′	x, y, z	2·762 (3)	1·95 (3)	155· (3)
OW2	HW2B	OW1	$x, y-1, z$	2·805 (2)	2·01 (4)	168· (4)
(4)						
C3′	H3′	O2′	$2-x, 0·5+y, 1·5-z$	3·239 (2)	2·27 (2)	165· (2)
O2′	HO2′	O5′	$1+x, y, z$	2·715 (2)	1·87 (2)	172· (2)
O3′	HO3′	N7	$2-x, 0·5+y, 1·5-z$	2·961 (2)	2·16 (3)	164· (2)
O5′	HO5′	O3′	$1-x, 0·5+y, 1·5-z$	2·745 (2)	1·96 (3)	170· (3)

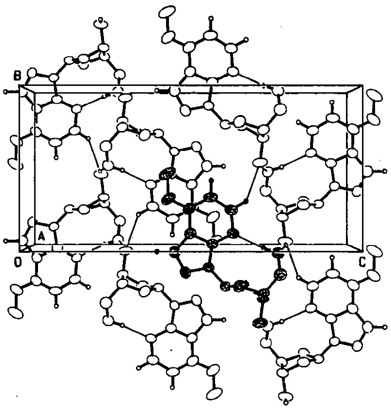

Fig. 5. Unit-cell projection of (1) viewed along the *a* axis. A single molecule has been shaded. Sugar CH hydrogens have been omitted for clarity. Hydrogen bonds are indicated by thin lines.

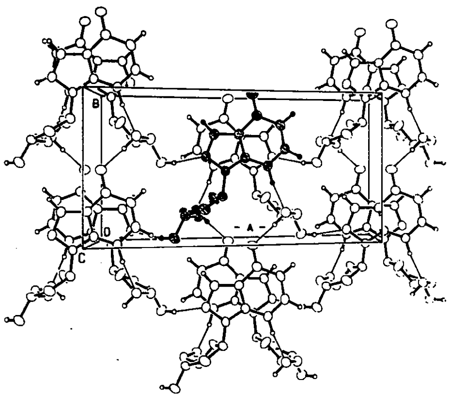

Fig. 6. Unit-cell projection of (2) viewed approximately perpendicular to the base plane of the shaded molecule. Sugar CH hydrogens have been omitted for clarity. Hydrogen bonds are indicated by thin lines.

which the ribose moieties reside. The interplanar spacing of the rings is about 3·4 Å [closest contact is C3···C6 of 3·387 (3) Å]. There is a very close intermolecular C3′—H3′···O2′ contact linking sugar moieties along the *b* axis; this is the only manner in which O2′ acts as a proton acceptor. The O3′—H···N7 and O5′—H···O3′ interactions also link molecules along the *b* axis whereas the O2′—H···O5′ hydrogen bonding binds molecules translated along the *a* axis, skipping the 2_1-related molecules. Thus, the structure along the *c* axis is bound only by the zipper-like base stacking interactions (illustrated in

Fig. 8*b*), a feature resulting from the absence of hydrogen-bondable functions on the base ring opposite the ribose moiety.

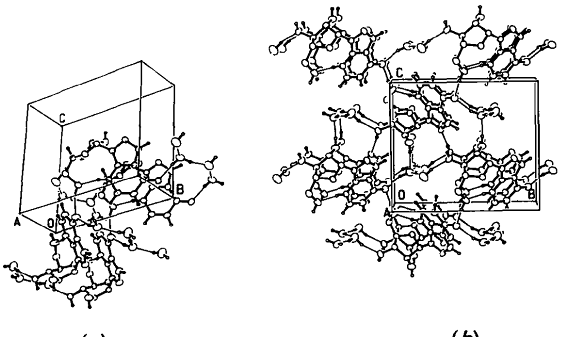
(*a*) (*b*)

Fig. 7. (*a*) Unit-cell projection of (3) viewed perpendicular to the base plane of the shaded molecule. Sugar CH hydrogens have been omitted. Hydrogen bonds are indicated by thin lines. (*b*) Unit-cell projection viewed approximately along the *a* axis illustrating the channel occupied by the hydrogen-bonded chain of water molecules.

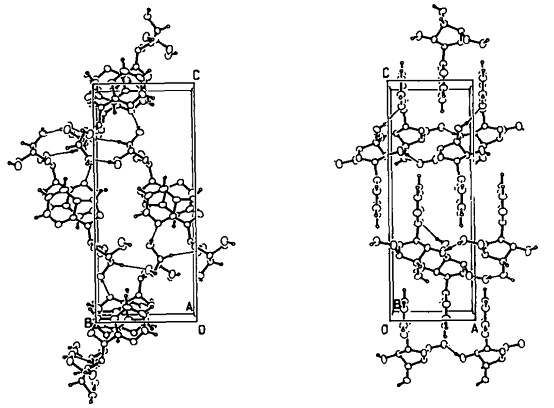
(*a*) (*b*)

Fig. 8. Packing diagrams of unit cell of (4). Sugar CH hydrogens (except H3′) have been omitted. Hydrogen bonds are indicated by thin lines. (*a*) Projection along the *a* axis illustrating the base stacking and high degree of overlap. (*b*) Projection along the *b* axis showing the zipper-like base stacking and the lack of hydrogen bonding interactions in the *c* direction.

References

Altona, C. & Sundaralingam, M. (1972). *J. Am. Chem. Soc.* **94**, 8205–8212.

Cline, B. L., Panzica, R. P. & Townsend, L. B. (1978). *J. Org. Chem.* **43**, 4910–4915.

Cordes, A. W. (1983). Personal communication.

Cottam, H. B., Petrie, C. R., McKernan, P. A., Goebel, R. J., Dalley, N. K., Davidson, R. B., Robins, R. K. & Revankar, G. R. (1984). *J. Med. Chem.* **27**, 1119–1127.

Cristalli, G., Franchetti, P., Grifantini, M., Vittori, S., Bordoni, T. & Geroni, C. (1987). *J. Med. Chem.* **30**, 1686–1688.

Cristalli, G., Franchetti, P., Grifantini, M., Vittori, S., Klotz, K.-N. & Lohse, M. J. (1988). *J. Med. Chem.* **31**, 1179–1183.

Frenz, B. A. (1985). *Enraf–Nonius SDP-Plus Structure Determination Package*. Version 3.0. Enraf–Nonius, Delft, The Netherlands.

International Tables for X-ray Crystallography (1974). Vol. IV. Birmingham: Kynoch Press. (Present distributor Kluwer Academic Publishers, Dordrecht.)

Itoh, T., Kitano, S. & Mizuno, Y. (1972). *J. Heterocycl. Chem.* **9**, 465–470.

Johnson, C. K. (1976). *ORTEP*II. Report ORNL-5138. Oak Ridge National Laboratory, Tennessee, USA.

Lichtenthaler, F. W. & Cuny, E. (1981). *Chem. Ber.* **114**, 1610–1623.

Meyer, R. B. Jr, Revankar, G. R., Cook, P. D., Ehler, K. W., Schweizer, M. P. & Robins, R. K. (1980). *J. Heterocycl. Chem.* **17**, 159–169.

Revankar, G. R., Gupta, P. K., Adams, A. D., Dalley, N. K., McKernan, P. A., Cook, P. D., Canonico, P. G. & Robins, R. K. (1984). *J. Med. Chem.* **27**, 1389–1396.

Sanghvi, Y. S., Larson, S. B., Willis, R. C., Robins, R. K. & Revankar, G. R. (1989). *J. Med. Chem.* **32**, 945–951.

Sheldrick, G. M. (1976). *SHELX76*. Program for crystal structure determination. Univ. of Cambridge, England.

Sheldrick, G. M. (1986). *SHELXS86*. Program for crystal structure solution. Univ. of Göttingen, Federal Republic of Germany.

Stewart, R. F., Davidson, E. R. & Simpson, W. T. (1965). *J. Chem. Phys.* **42**, 3175–3187.

Acta Cryst. (1990). C**46**, 797–799

Isotypic Structures of (I) Tri(2-hydroxyethyl)ammonium Hydrogensulfide and (II) Tri(2-hydroxyethyl)ammonium Chloride

By Dietrich Mootz, Dieter Brodalla and Michael Wiebcke

Institut für Anorganische Chemie und Strukturchemie, Heinrich-Heine-Universität Düsseldorf, Universitätsstraße 1, *D*-4000 *Düsseldorf, Federal Republic of Germany*

(*Received* 26 *July* 1989; *accepted* 14 *August* 1989)

Abstract. (I) $[\mathrm{NH(CH_2CH_2OH)_3}]\mathrm{HS}$, $M_r = 183{\cdot}27$, trigonal, $R3c$, $a = 8{\cdot}394\,(2)$, $c = 23{\cdot}513\,(4)$ Å, $V = 1434{\cdot}8$ Å^3, $Z = 6$, $D_x = 1{\cdot}27$ Mg m^{-3}, $\lambda(\mathrm{Mo}\ K\bar{\alpha}) = 0{\cdot}71069$ Å, $\mu = 0{\cdot}291$ mm^{-1}, $F(000) = 600$, room temperature, $R = 0{\cdot}022$ for 278 unique observed reflections. (II) $[\mathrm{NH(CH_2CH_2OH)_3}]\mathrm{Cl}$, $M_r = 185{\cdot}65$,

0108-2701/90/050797-03$03.00